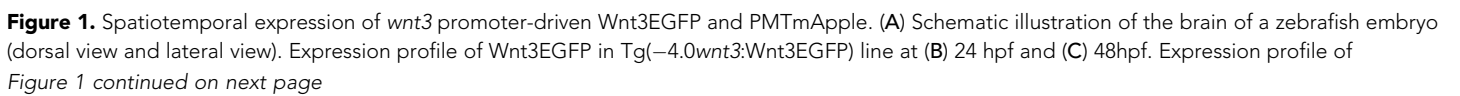


---

## Figures and figure supplements

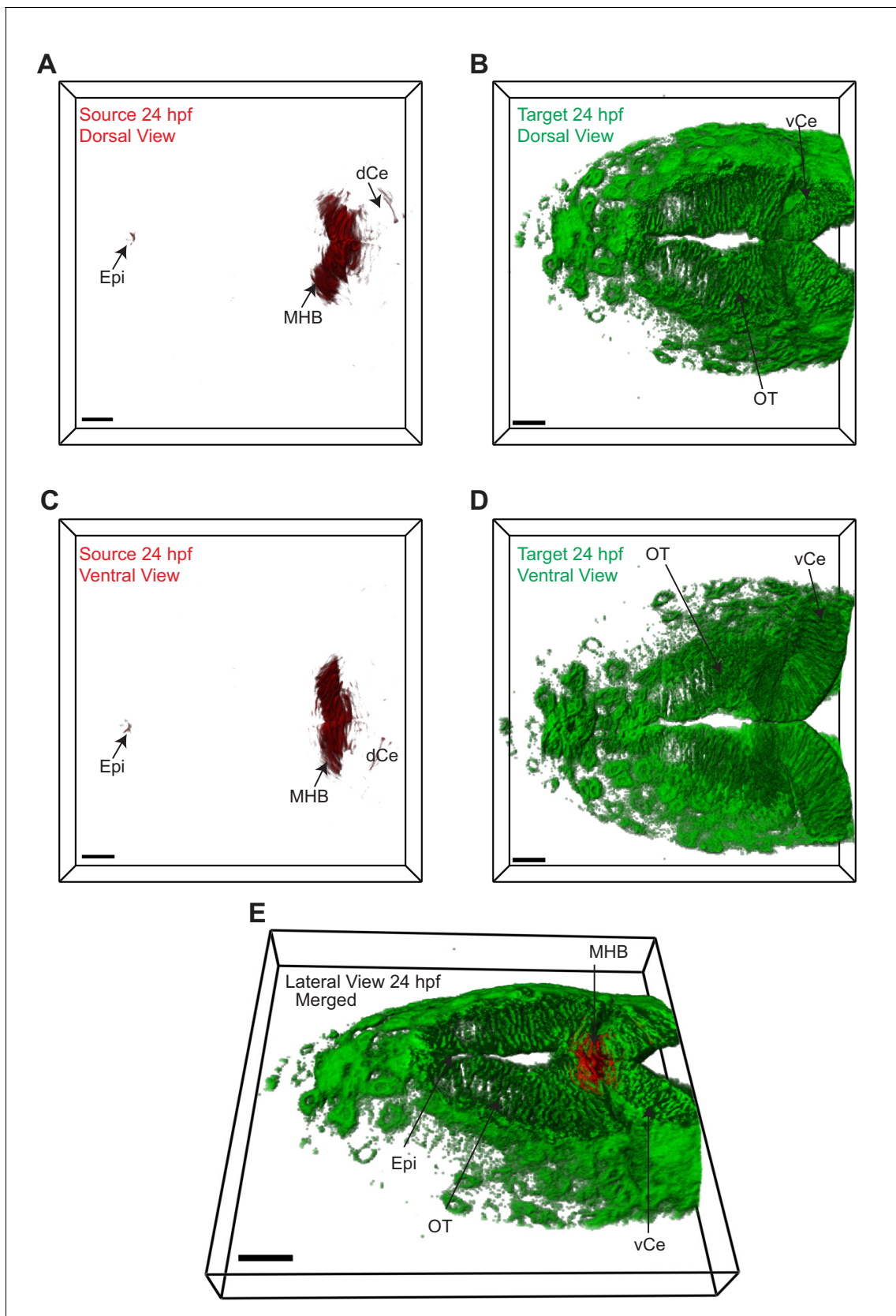
Wnt3 distribution in the zebrafish brain is determined by expression, diffusion and multiple molecular interactions

**Sapthaswaran Veerapathiran *et al***



*Figure 1 continued*

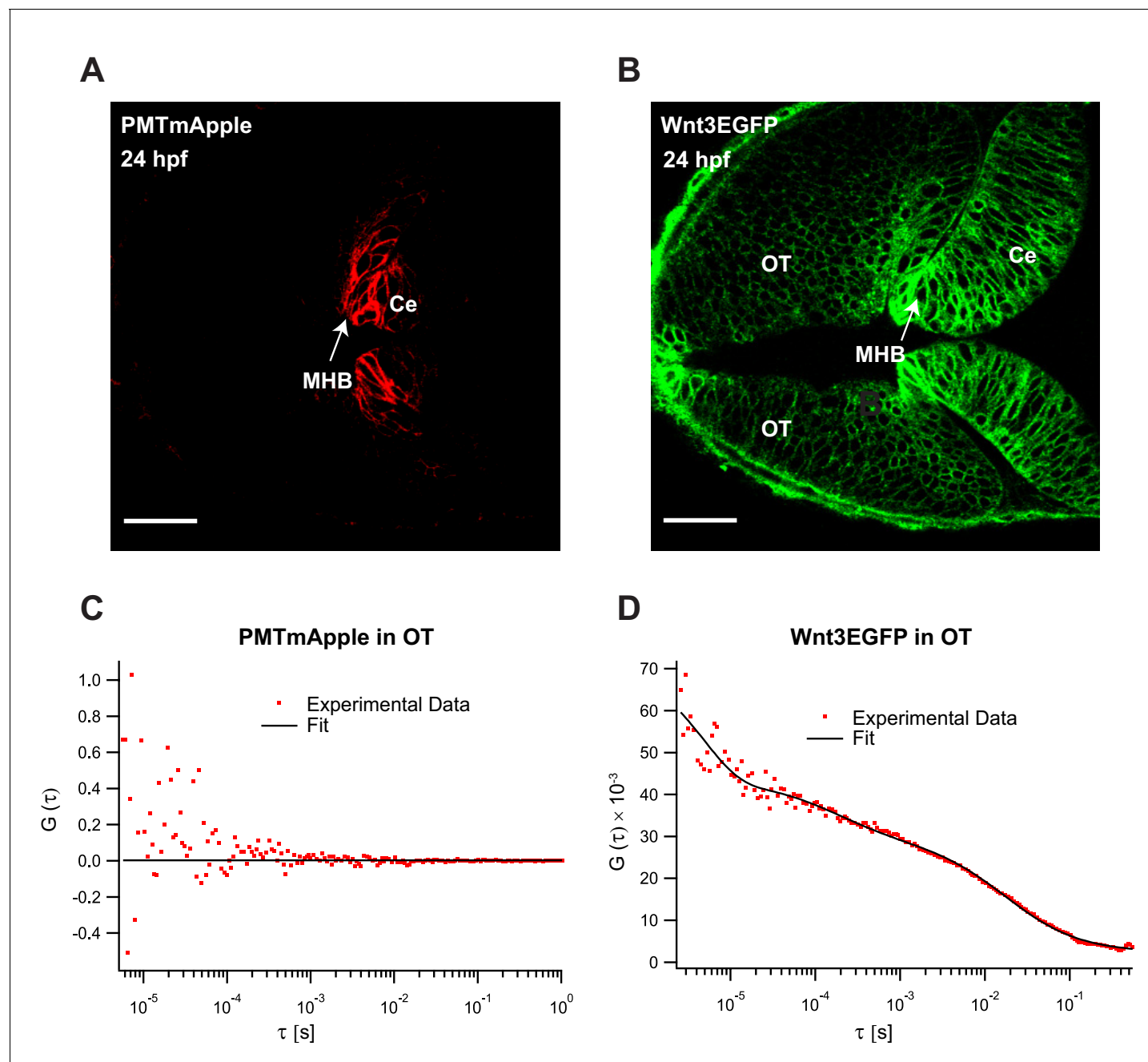
PMTmApple in Tg(−4.0wnt3:PMTmApple) line at (D) 24 hpf and (E) 48hpf. BV, brain ventricle; Ce, cerebellum; CP, choroid plexus; E, epiphysis; FP, floor plate; HB, hindbrain; MHB, midbrain–hindbrain boundary; mRP, midbrain roof plate; OT, optic tectum; r, rhombomere; RP, roof plate (spinal cord); SCO, sub-commissural organ. SCO and E are regions of the epithalamus (Epi). Images orientation: anterior to the left. Scale bar 30  $\mu$ m.



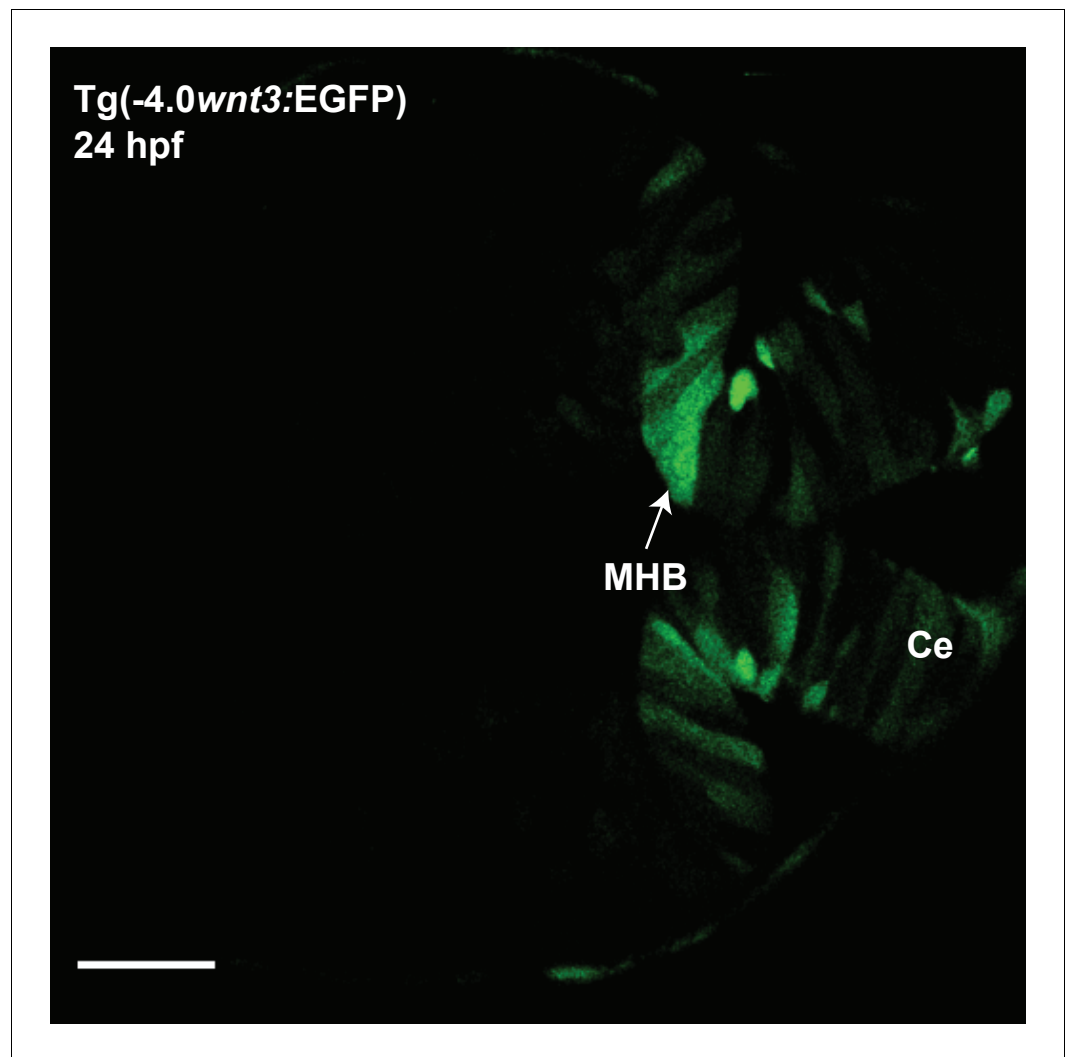
**Figure 2.** Wnt3 source and target regions at 24 hpf. 3D dorsal projection of Wnt3 (A) source regions at 24 hpf and (B) target regions at 24 hpf (top view). 3D ventral projection of Wnt3 (C) source regions at 24 hpf and (D) target regions at 24 hpf (bottom view). (E) 3D projection of Wnt3 source and target regions at 24 hpf. *Figure 2 continued on next page*

*Figure 2 continued*

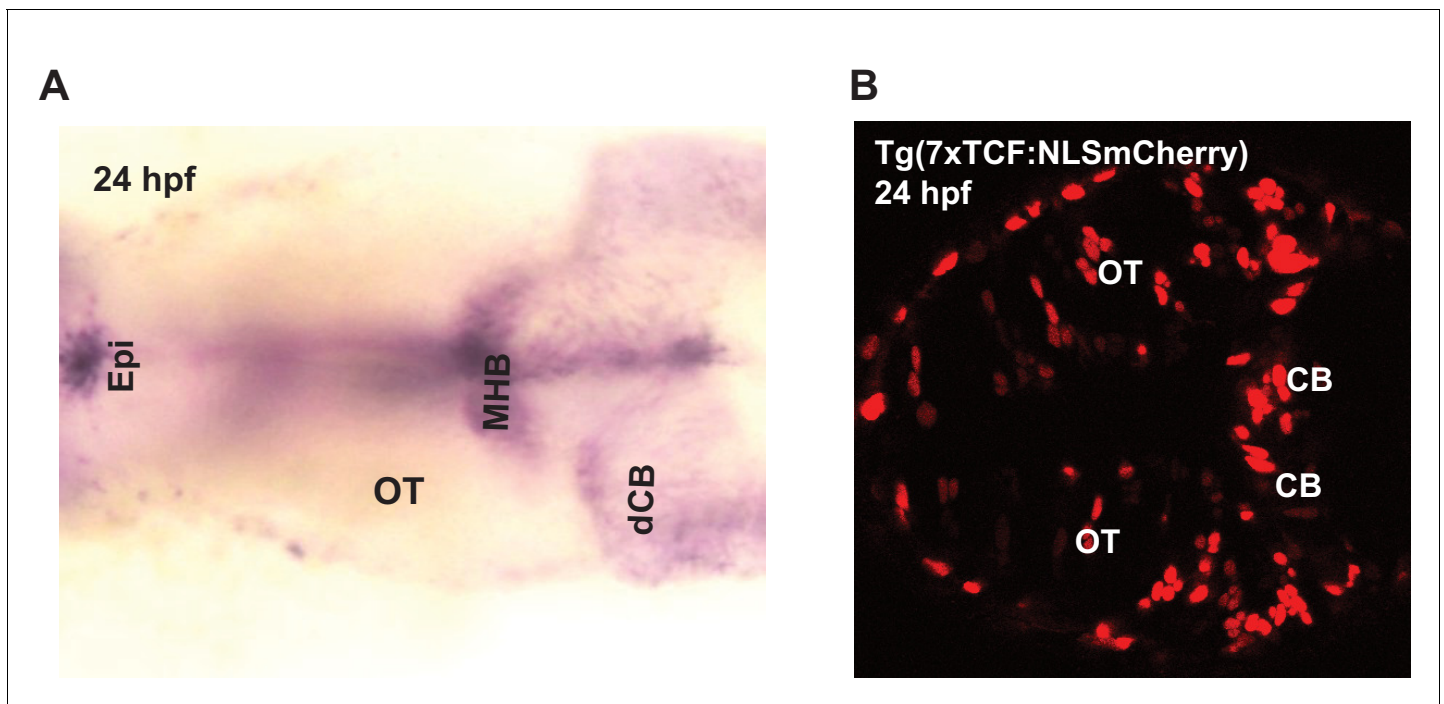
target regions at 24 hpf (lateral view). See **Video 3** for a detailed view. dCe, dorsal regions of cerebellum; Epi, epithalamus; MHB, midbrain–hindbrain boundary; OT, optic tectum; vCe, ventral regions of cerebellum. Images orientation: anterior to the left. Scale bar 30  $\mu$ m.



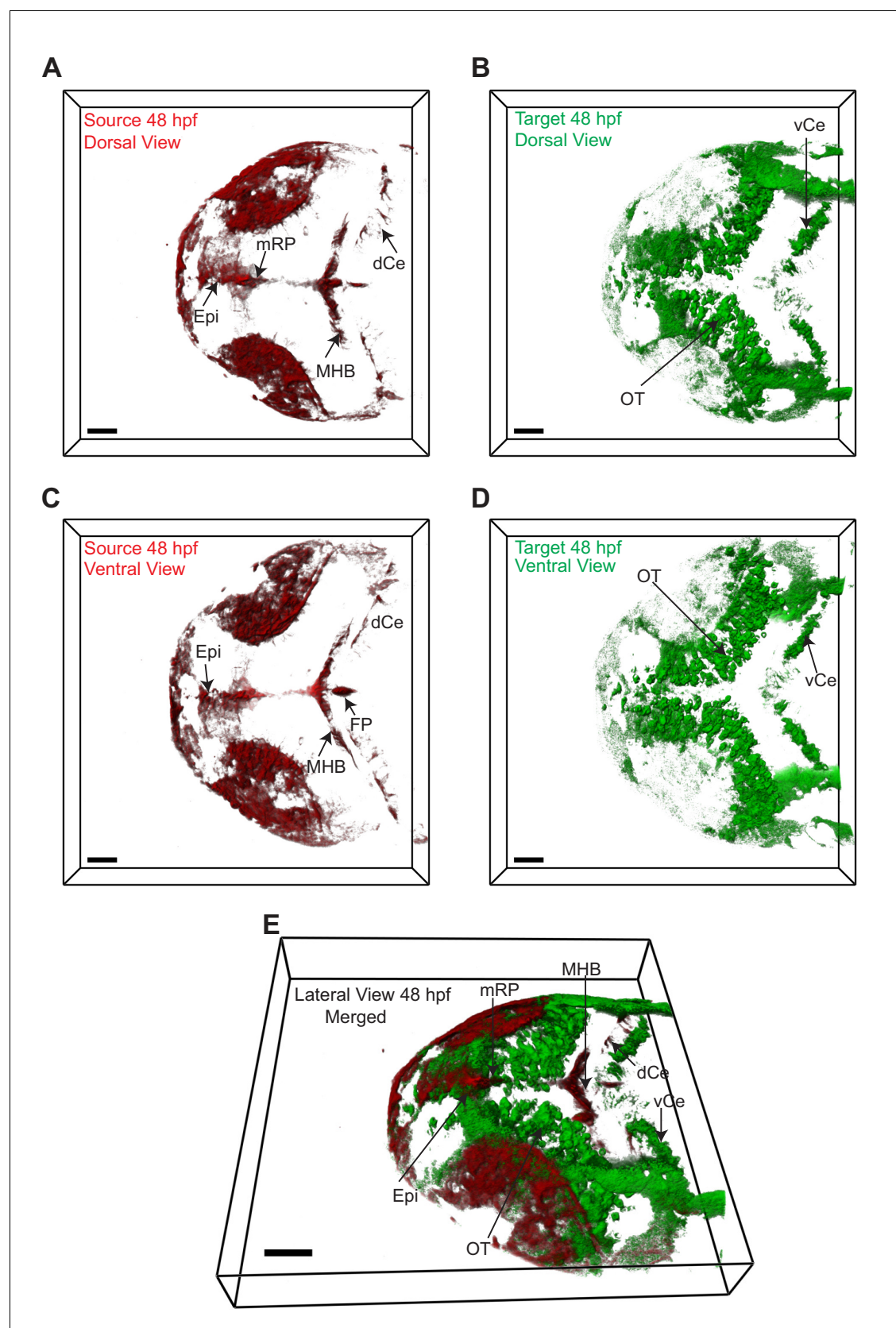
**Figure 2—figure supplement 1.** Fluorescence correlation spectroscopy (FCS) measurements of Wnt3EGFP and PMTmApple in the Wnt3 target regions at 24 hpf. Expression of (A) PMTmApple and (B) Wnt3EGFP in  $Tg(-4.0wnt3:Wnt3EGFP) \times Tg(-4.0wnt3:PMTmApple)$  double transgenic embryos at 24 hpf. Representative autocorrelation function (ACF) for (C) PMTmApple and (D) Wnt3EGFP in the OT at 24 hpf. No ACFs were obtained for PMTmApple in the target regions indicating an absence of mApple signal in these regions. Ce, cerebellum; MHB, midbrain–hindbrain boundary; OT, optic tectum. Images orientation: anterior to the left. Scale bar 30  $\mu m$ .



**Figure 2—figure supplement 2.** Expression of EGFP in Tg(-4.0wnt3:EGFP) at 24 hpf. The expression of EGFP in Tg(-4.0wnt3:EGFP) closely mimics the expression of PMTmApple in Tg(-4.0wnt3:PMTmApple). Ce, cerebellum; MHB; midbrain–hindbrain boundary. Images orientation: anterior to the left. Scale bar 30  $\mu$ m.



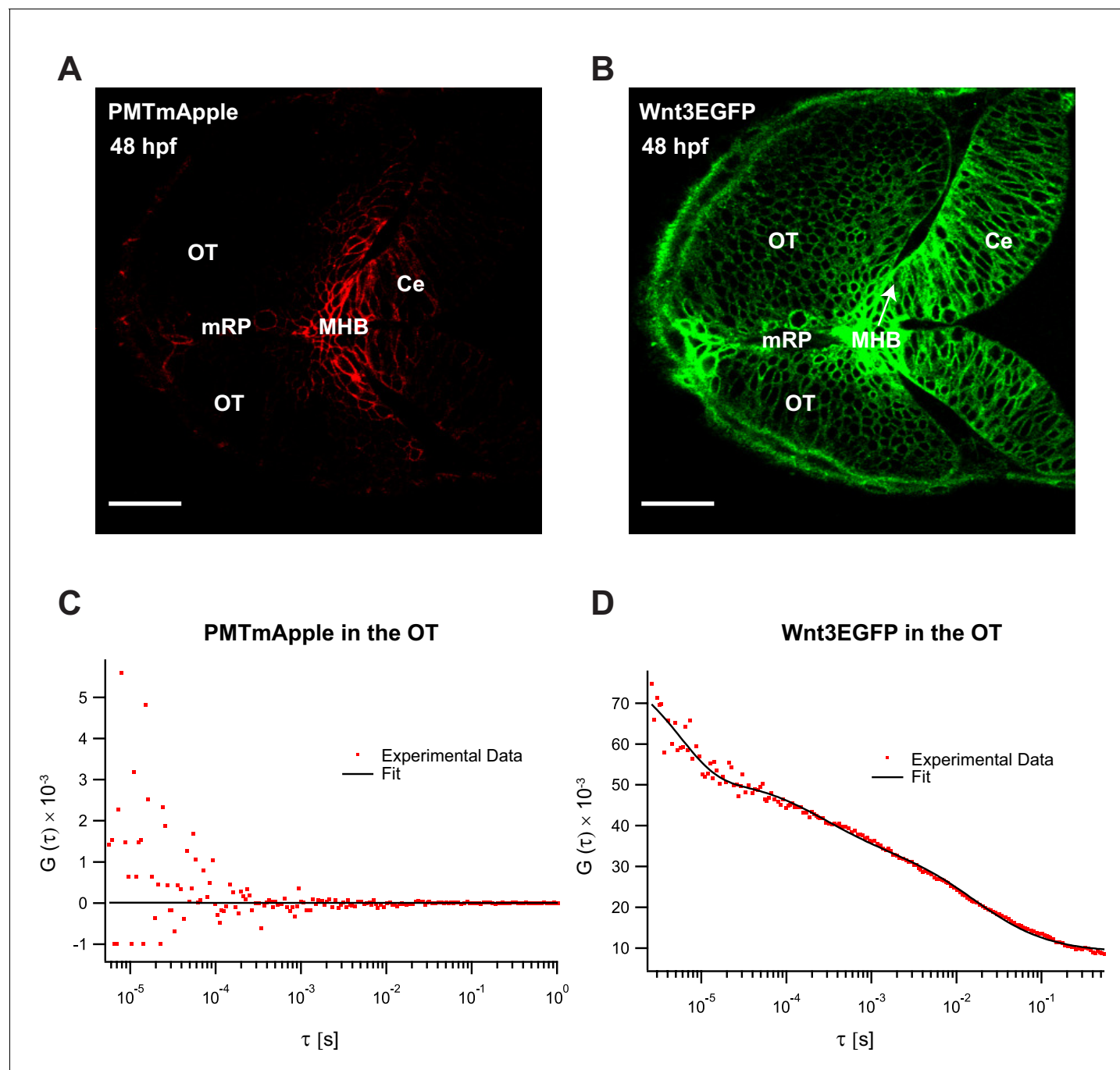
**Figure 2—figure supplement 3.** Expression of *wnt3* transcripts and downstream *wnt* signaling transcription factor at 24 hpf. (A) Whole mount in situ hybridization (dorsal view) of *wnt3* at 24 hpf. The expression pattern is similar to previously published results in *Clements et al., 2009*, *Duncan et al., 2015*, and *Teh et al., 2015*. (B) Expression of NLS-mCherry in *wnt* reporter line *Tg(7xTCF-Xla.Siam:NLS-Cherry)* at 24 hpf. dCB, cerebellum; Epi, epithalamus; FP, floor plate; MHB, midbrain–hindbrain boundary; mRP, midbrain roof plate; OT, optic tectum. Orientation: anterior to left.



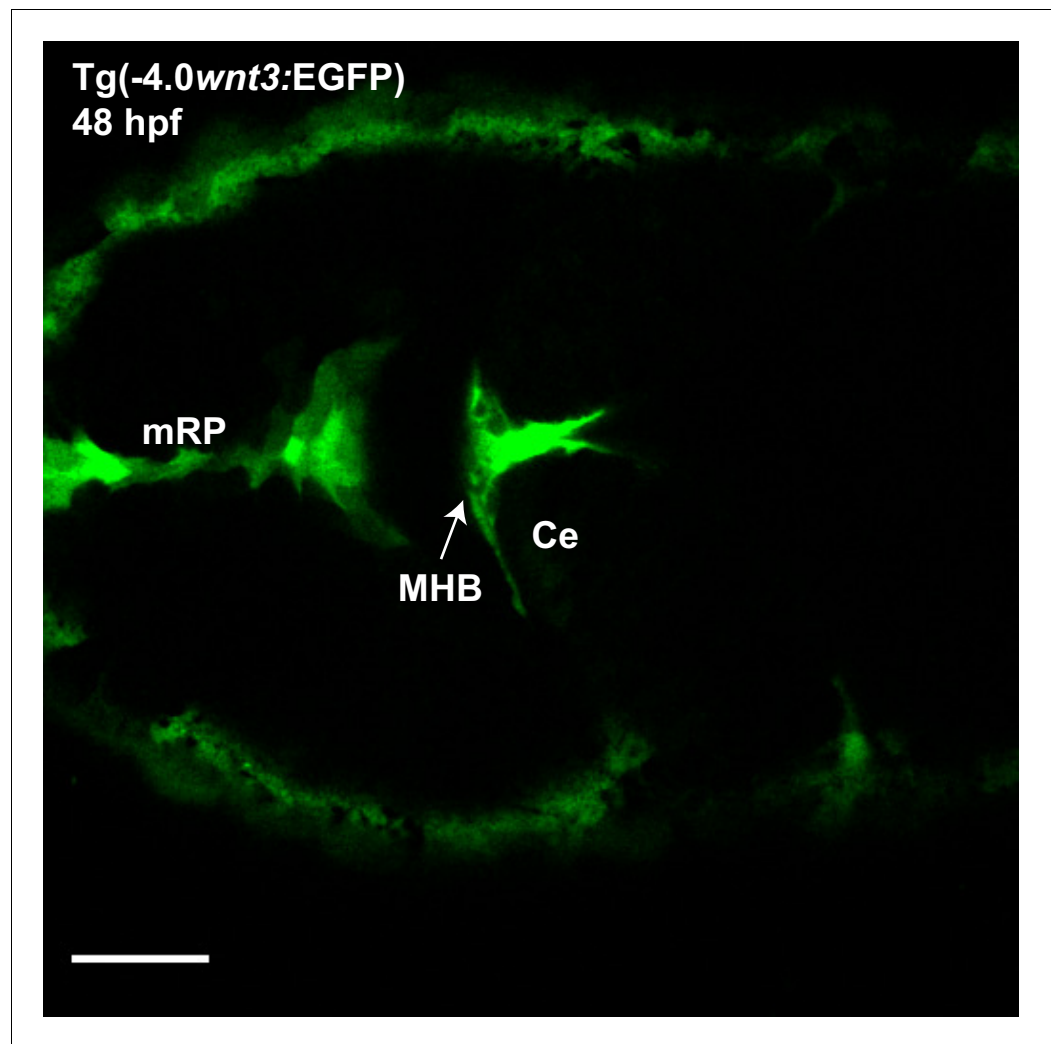
**Figure 3.** Wnt3 source and target regions at 48 hpf. 3D dorsal projection of Wnt3 (A) source regions at 48 hpf and (B) target regions at 48 hpf (top view). 3D ventral projection of Wnt3 (C) source regions at 48 hpf and (D) target regions at 48 hpf (bottom view). (E) 3D projection of Wnt3 source and target regions at 48 hpf. Figure 3 continued on next page

Figure 3 continued

target regions at 48 hpf (lateral view). See **Video 4** for a detailed view. dCe, dorsal regions of cerebellum; Epi, epithalamus; FP, floor plate; MHB, midbrain–hindbrain boundary; mRP, midbrain roof plate; OT, optic tectum; vCe, ventral regions of cerebellum. Images orientation: anterior to the left. Scale bar 40  $\mu$ m.



**Figure 3—figure supplement 1.** Fluorescence correlation spectroscopy (FCS) measurements of Wnt3EGFP and PMTmApple in the Wnt3 target regions at 48 hpf. Expression of (A) PMTmApple and (B) Wnt3EGFP in  $Tg(-4.0wnt3:Wnt3EGFP) \times Tg(-4.0wnt3:PMTmApple)$  double transgenics at 48 hpf. Representative autocorrelation function (ACF) for (C) PMTmApple and (D) Wnt3EGFP in the OT at 48 hpf. No ACFs were obtained for PMTmApple in the target regions indicating an absence of mApple signal in these regions. Ce, cerebellum; MHB, midbrain–hindbrain boundary; OT, optic tectum. Images orientation: anterior to the left. Scale bar 30  $\mu m$ .



**Figure 3—figure supplement 2.** Expression of EGFP in Tg(-4.0wnt3:EGFP) at 48 hpf. The expression of EGFP in Tg(-4.0wnt3:EGFP) closely mimics the expression of PMTmApple in Tg(-4.0wnt3:PMTmApple). Ce, cerebellum; MHB, midbrain-hindbrain boundary; OT, optic tectum. Images orientation: anterior to the left. Scale bar 30  $\mu$ m.

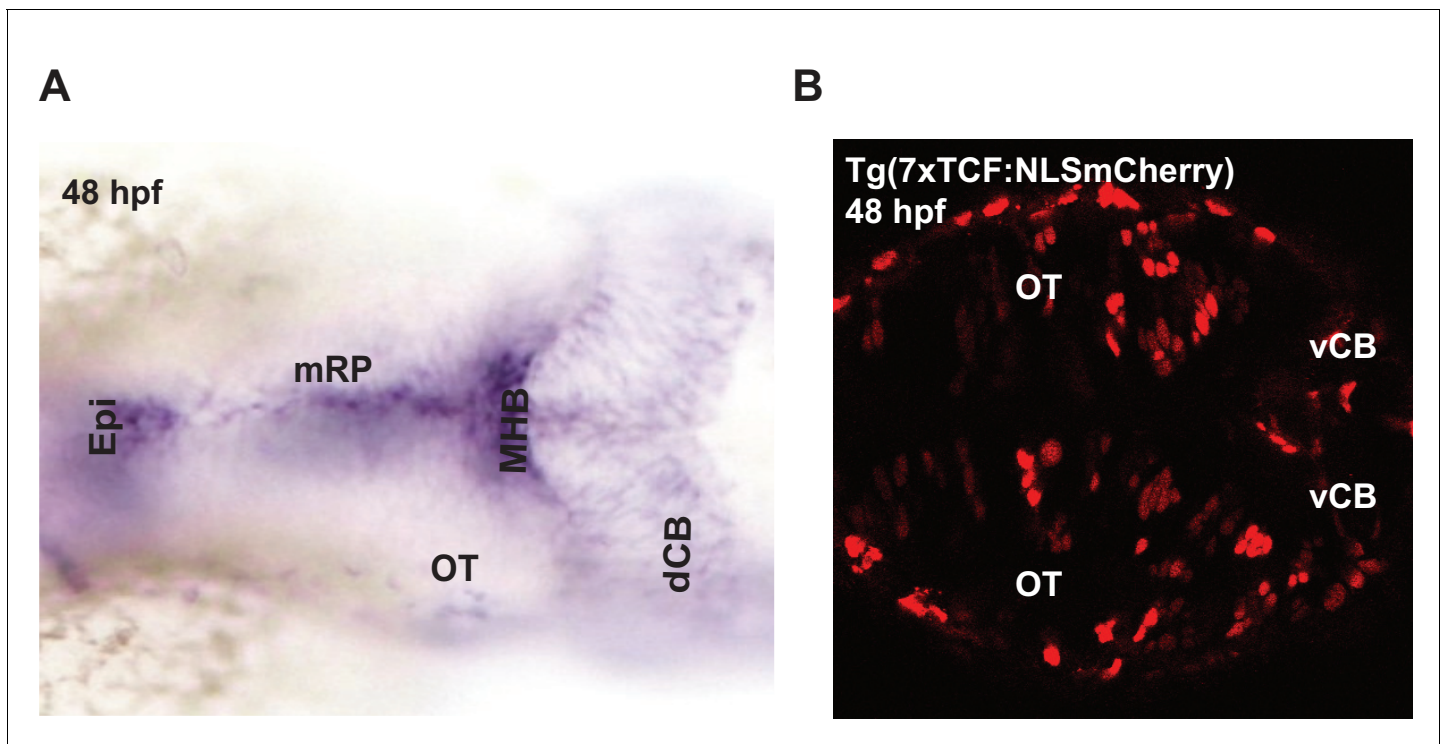


**Figure 3—figure supplement 3.** Expression of *wnt3* transcripts and downstream wnt signaling transcription factors at 48 hpf. (A) Whole mount in situ hybridization (dorsal view) of *wnt3* at 48 hpf. The expression pattern is similar to previously published results in *Clements et al., 2009*, *Duncan et al., 2015*, and *Teh et al., 2015*. (B) Expression of NLS-mCherry in wnt reporter line Tg(7xTCF-Xla.Siam:NLS-Cherry) at 48 hpf. dCB, cerebellum; Epi, epithalamus; FP, floor plate; MHB, midbrain–hindbrain boundary; mRP, midbrain roof plate; OT, optic tectum. Orientation: anterior to left.

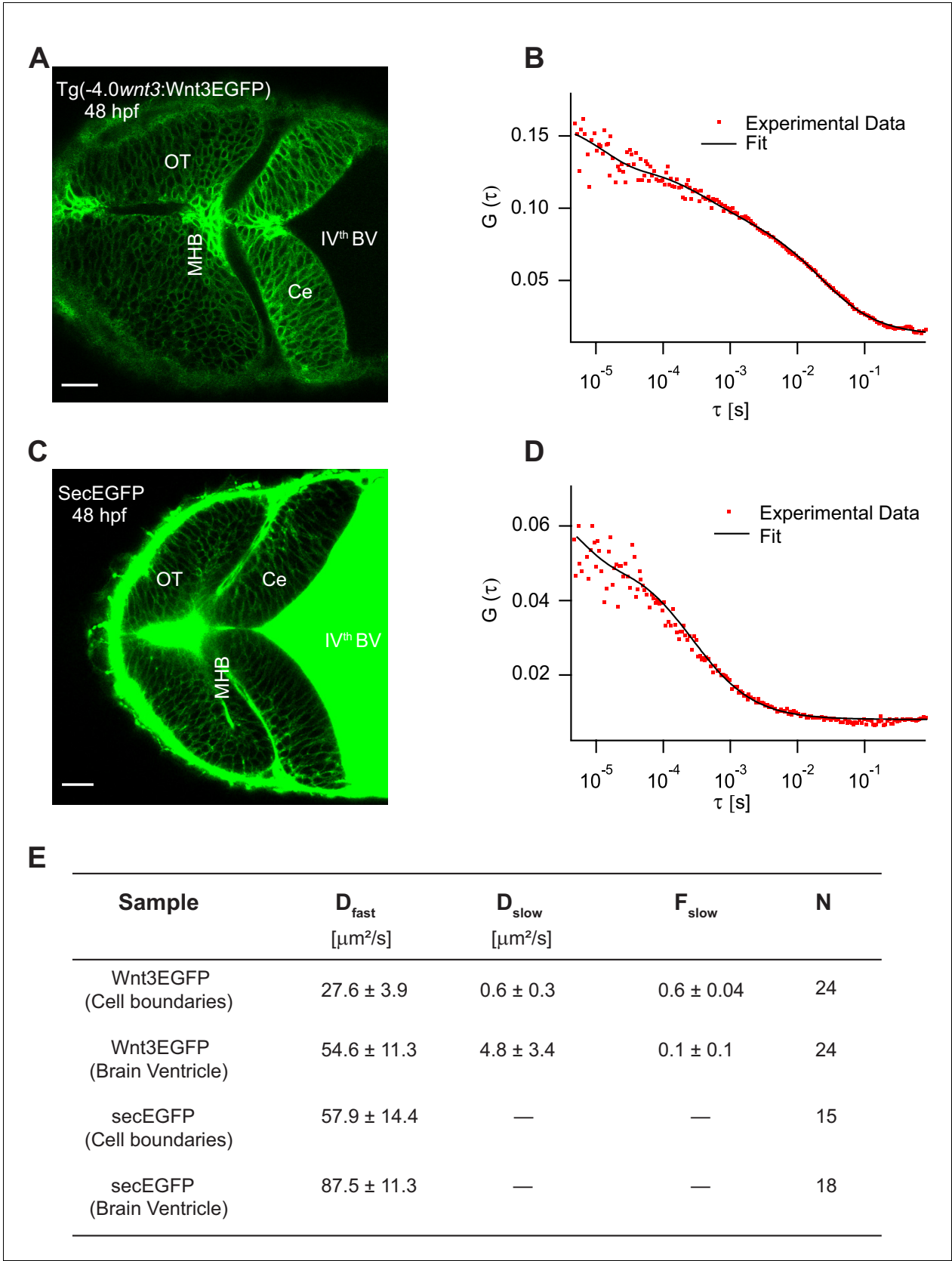


**Figure 4.** Characterizing the dynamics of Wnt3EGFP and secEGFP using fluorescence correlation spectroscopy (FCS). (A) Expression of Wnt3EGFP in Tg(−4.0wnt3:Wnt3EGFP) at 48 hpf. (B) Representative autocorrelation function (ACF; dots) and fitting (line) of a Wnt3EGFP measurement at a cell

Figure 4 continued on next page

*Figure 4 continued*

boundary. (C) Expression of secEGFP in the zebrafish brain at 48 hpf. (D) Representative ACF (dots) and fitting (line) of a secEGFP measurement at a cell boundary. (E) Table showing diffusion coefficients of the fast component ( $D_{fast}$ ), slow component ( $D_{slow}$ ) and the fraction of slow component ( $F_{slow}$ ) for Wnt3EGFP and secEGFP measured by FCS. Measurements were performed in the cell borders of Ce, MHB, and OT; and in the BV. Data are mean  $\pm$  SD; N = No of measurements. BV, brain ventricle; Ce, cerebellum; MHB, midbrain–hindbrain boundary; OT, optic tectum. Images orientation: anterior to left. Scale bar 30  $\mu$ m.

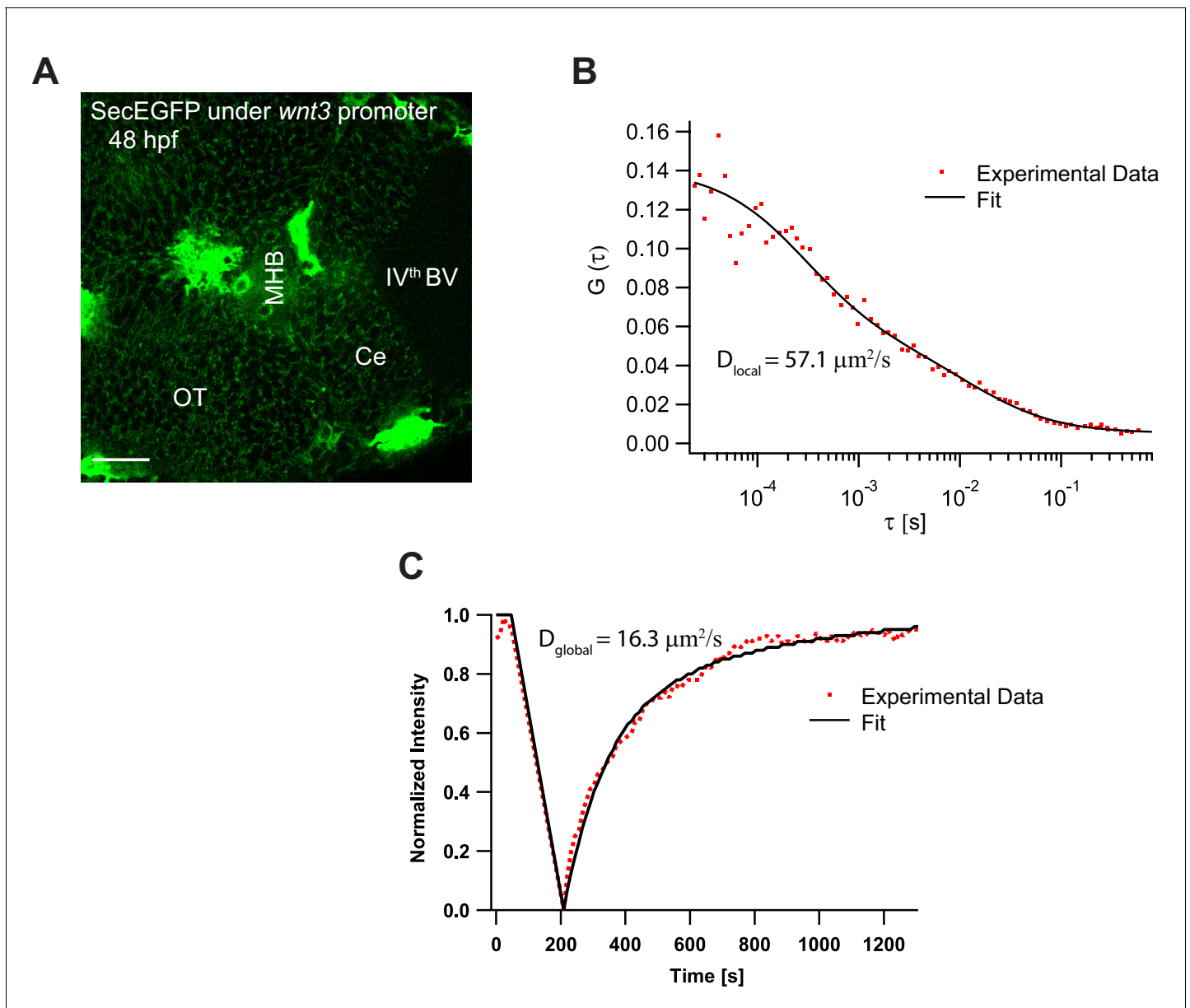


**Figure 4—figure supplement 1.** Expression and dynamics of secEGFP under 4 kb *wnt3* promoter. (A) Expression of secEGFP under *wnt3* promoter in the zebrafish brain at 48hpf. (B) Representative fluorescence correlation spectroscopy measurement of secEGFP under *wnt3* promoter with a diffusion coefficient of  $57.1 \mu\text{m}^2/\text{s}$ . (C) Representative fluorescence recovery after photobleaching recovery curve of secEGFP under *wnt3* promoter with a diffusion coefficient of  $16.3 \mu\text{m}^2/\text{s}$ . Orientation: anterior to the left. Scale bar 30 μm.

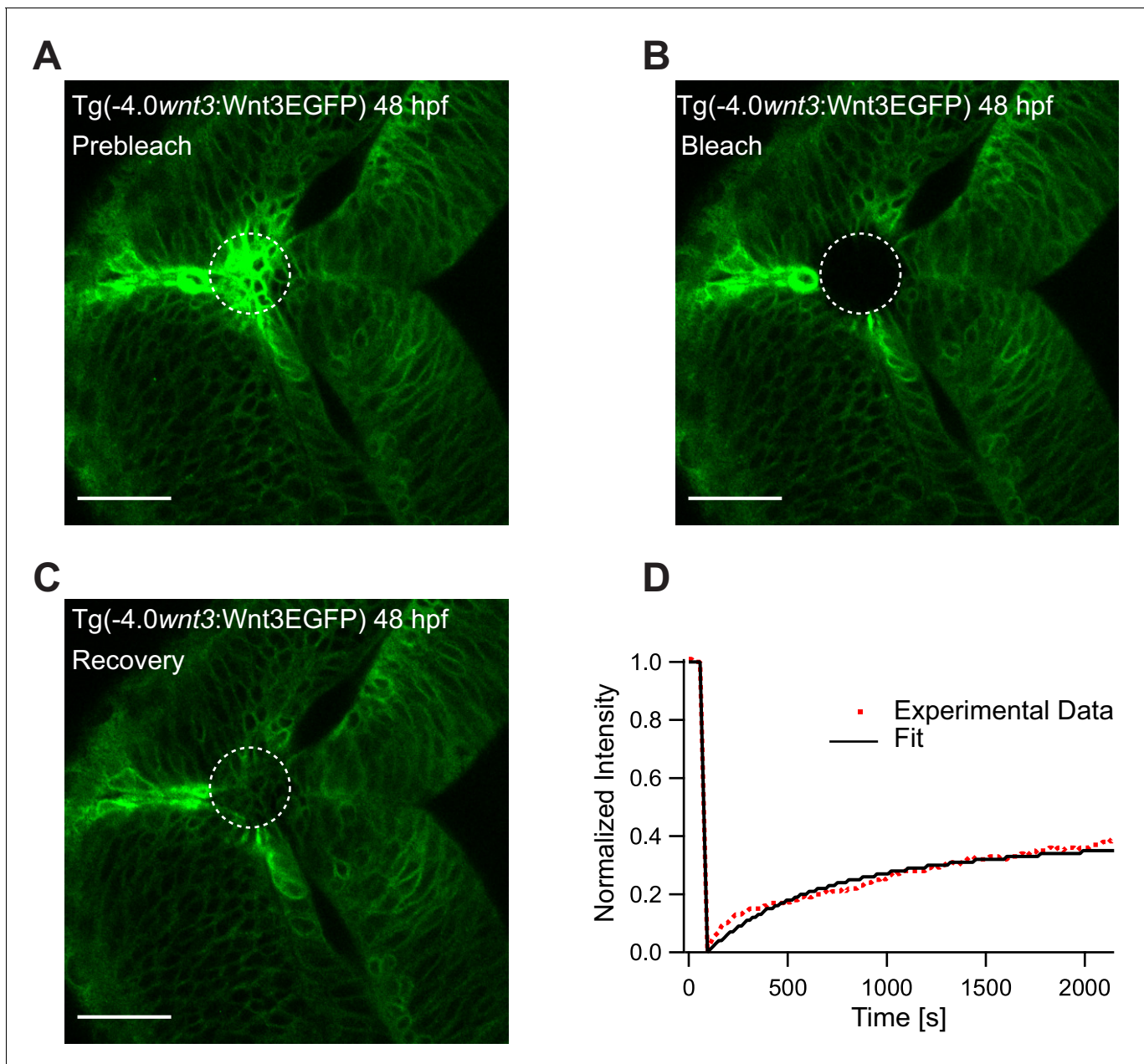


**Figure 5.** Representative fluorescence recovery of Wnt3EGFP at 48 hpf after photobleaching. (A) Expression of Wnt3EGFP in Tg(−4.0wnt3:Wnt3EGFP) at 48 hpf before photobleaching. (B) Photobleached region of Wnt3EGFP. (C) Recovery of fluorescence intensity in the bleached region due to diffusion of molecules from the neighboring unbleached regions. (D) Fluorescence recovery curve for Wnt3EGFP with a time constant ( $\tau_{\text{fast}}$ ) of ~5 min and a mobile component fraction ( $F_m$ ) of ~0.35. The average apparent global diffusion coefficient ( $D_{\text{global}}$ ) measured for Wnt3EGFP was  $0.5 \pm 0.2 \mu\text{m}^2/\text{s}$  ( $N = 11$ ). Fluorescence recovery after photobleaching for Wnt3EGFP at a distal target site showed similar recovery dynamics (**Figure 5—figure supplement 1**) whereas recovery after heparan sulfate proteoglycan disruption showed faster recovery (**Figure 5—figure supplement 2**). Orientation: anterior to the left. Scale bar 30  $\mu\text{m}$ .

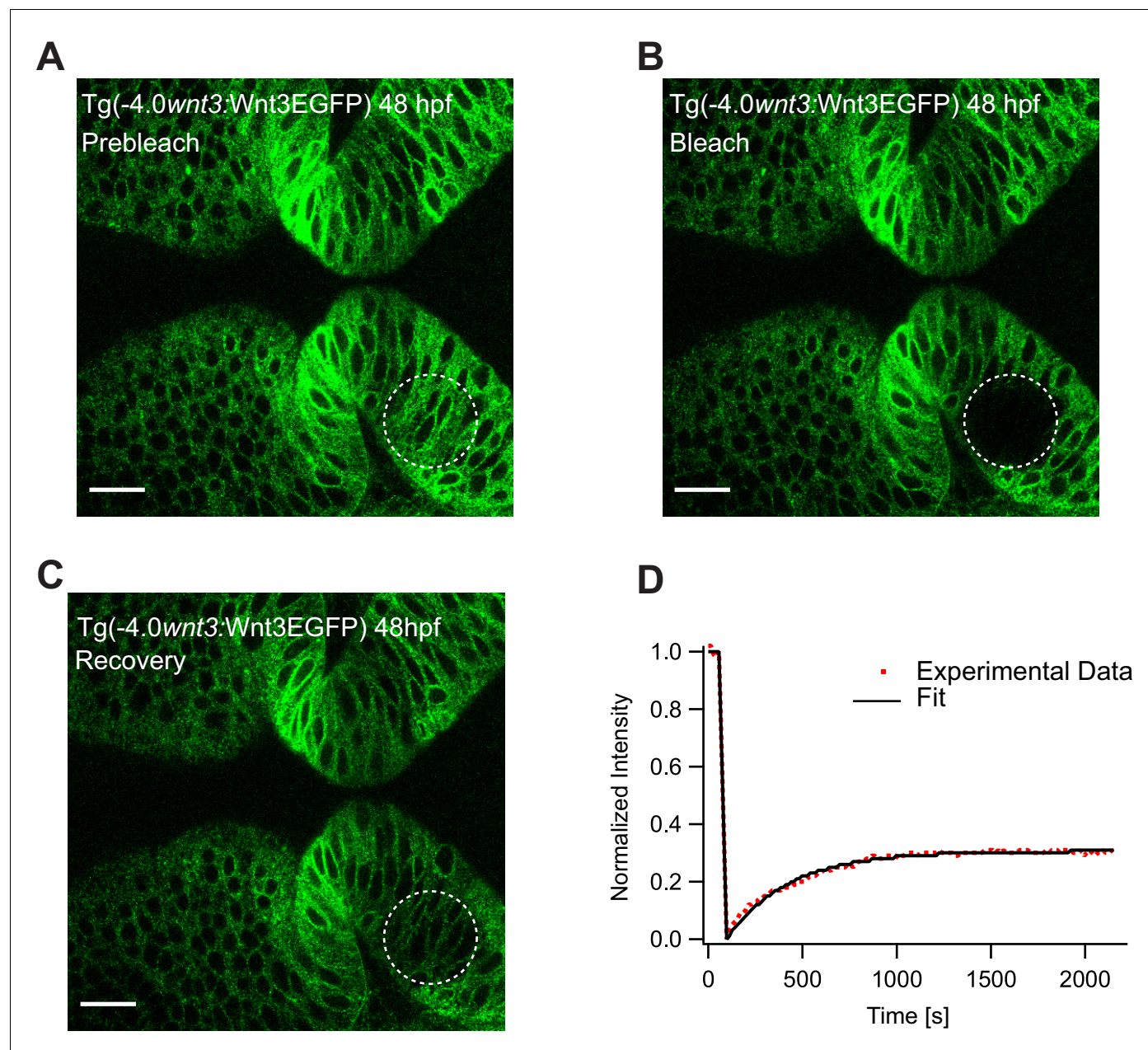


**Figure 5—figure supplement 1.** Representative fluorescence recovery of Wnt3EGFP at a distal target site after photobleaching. (A) Expression of Wnt3EGFP in Tg(-4.0wnt3:Wnt3EGFP) 48 hpf before photobleaching. (B) Photobleached region of Wnt3EGFP. (C) Recovery of fluorescence intensity in the bleached region due to diffusion of molecules from the neighboring unbleached regions. (D) Fluorescence recovery curve for Wnt3EGFP with a time constant ( $\tau_{\text{fast}}$ ) of ~6.5 min and an apparent global diffusion coefficient ( $D_{\text{global}}$ ) of 0.47  $\mu\text{m}^2/\text{s}$ . Scale bar 30  $\mu\text{m}$ .

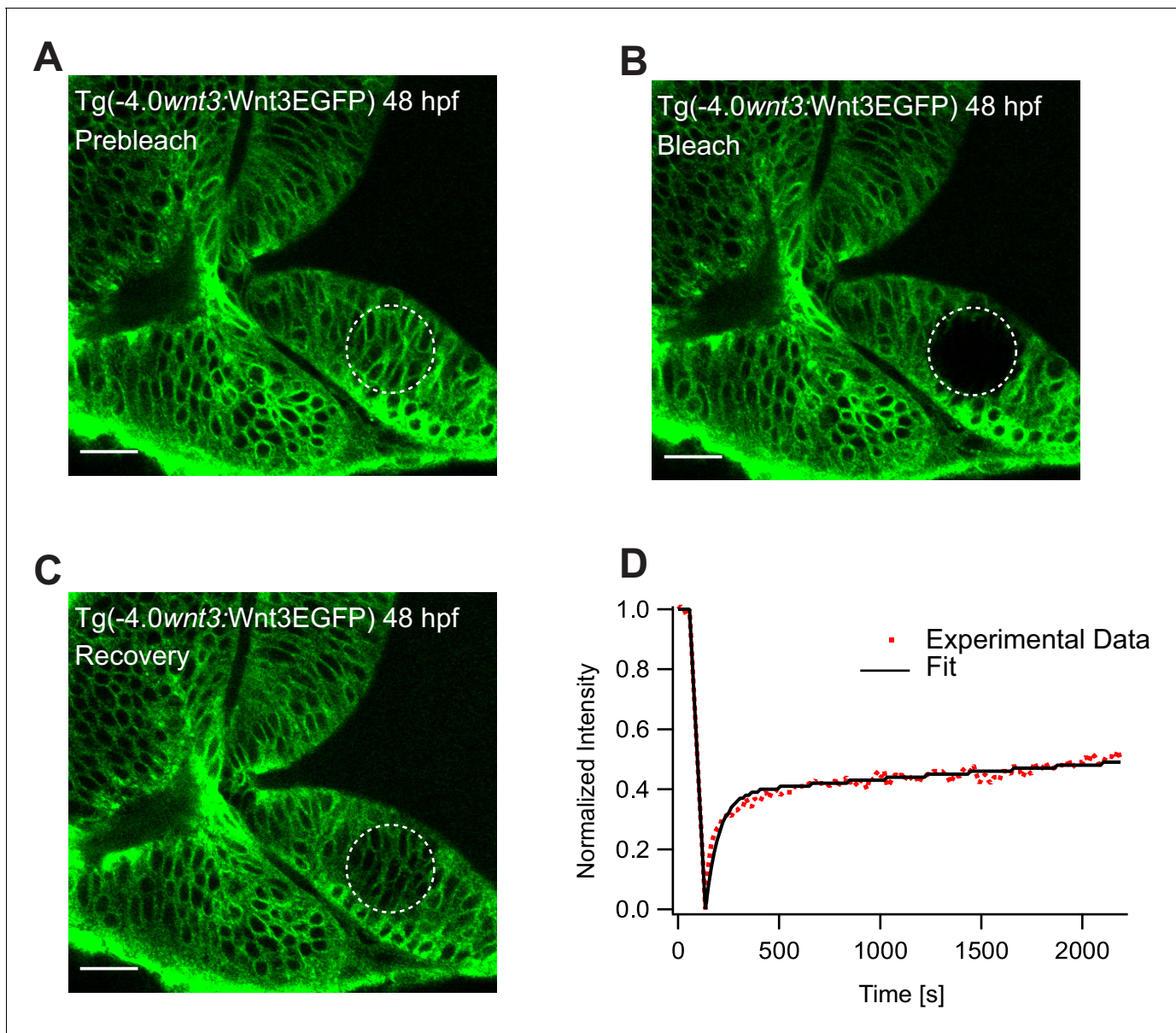


**Figure 5—figure supplement 2.** Representative fluorescence recovery of Wnt3EGFP at a distal target site after heparan sulfate proteoglycan (HSPG) disruption. (A) Expression of Wnt3EGFP in Tg(-4.0wnt3:Wnt3EGFP) before photobleaching in HSPG disrupted embryos. (B) Photobleached region of Wnt3EGFP. (C) Recovery of fluorescence intensity in the bleached region due to diffusion from the neighboring unbleached regions. (D) Fluorescence recovery curve for Wnt3EGFP with a recovery time ( $\tau_{fast}$ ) of ~1.5–2.5 min and a  $D_{global}$  of ~1.5–3.75  $\mu\text{m}^2/\text{s}$ , which is approximately two to three times faster than untreated embryos as shown in **Figure 5**. Images orientation: anterior to the left. Scale bar 30  $\mu\text{m}$ .

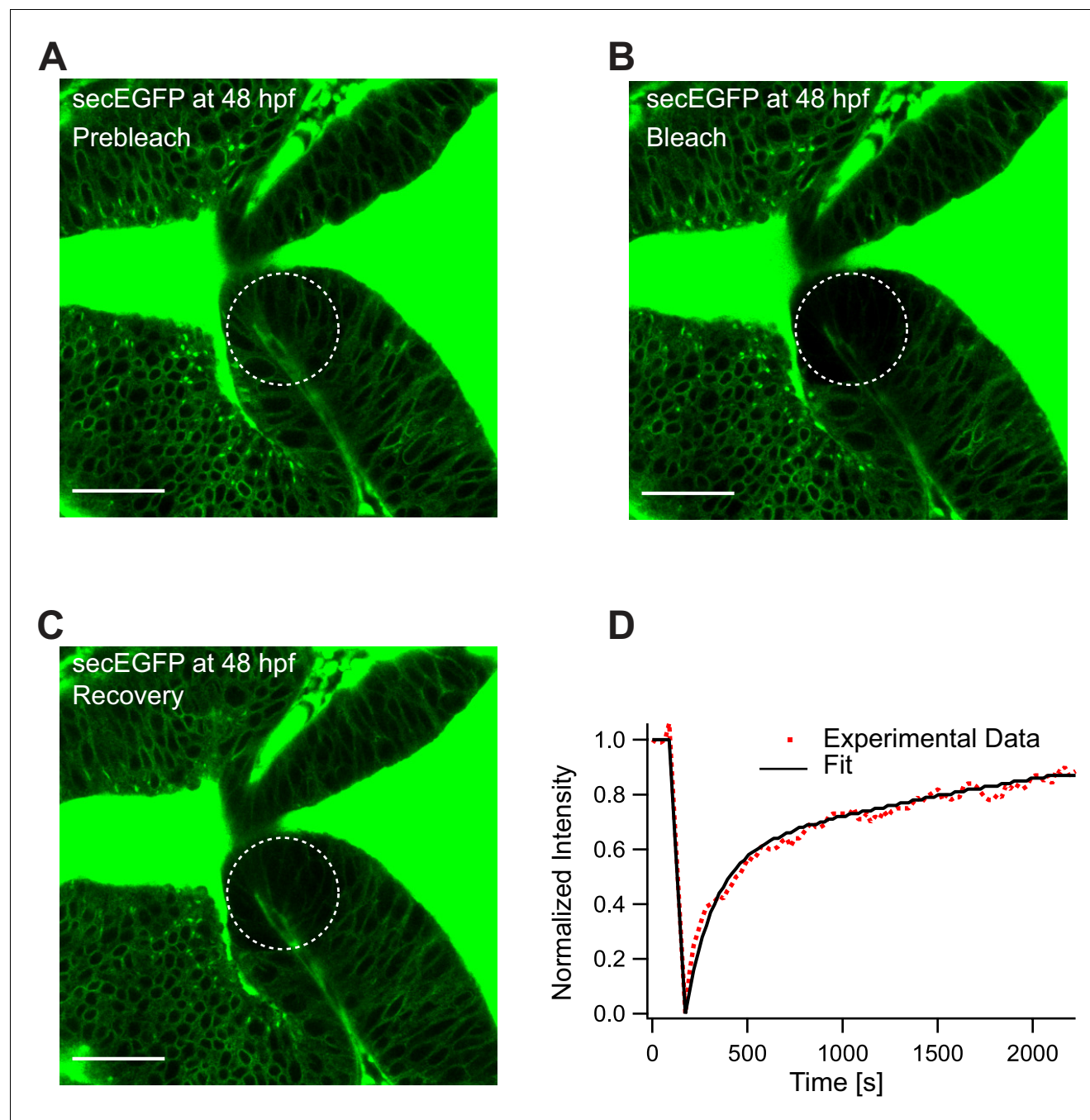


**Figure 5—figure supplement 3.** Representative fluorescence recovery of secEGFP after photobleaching at 48 hpf. (A) Expression of secEGFP before photobleaching. (B) Photobleached region of secEGFP. (C) Recovery of fluorescence intensity in the bleached region due to diffusion of molecules from the neighboring unbleached regions. (D) Fluorescence recovery curve for secEGFP with a quick recovery time ( $\tau_{\text{fast}}$ ) of ~45 s and a fraction of mobile component ( $F_m$ ) of ~0.85. The average global diffusion coefficient ( $D_{\text{global}}$ ) measured for secEGFP was  $13 \pm 4 \mu\text{m}^2/\text{s}$ . Images orientation: anterior to the left. Scale bar 30  $\mu\text{m}$ .

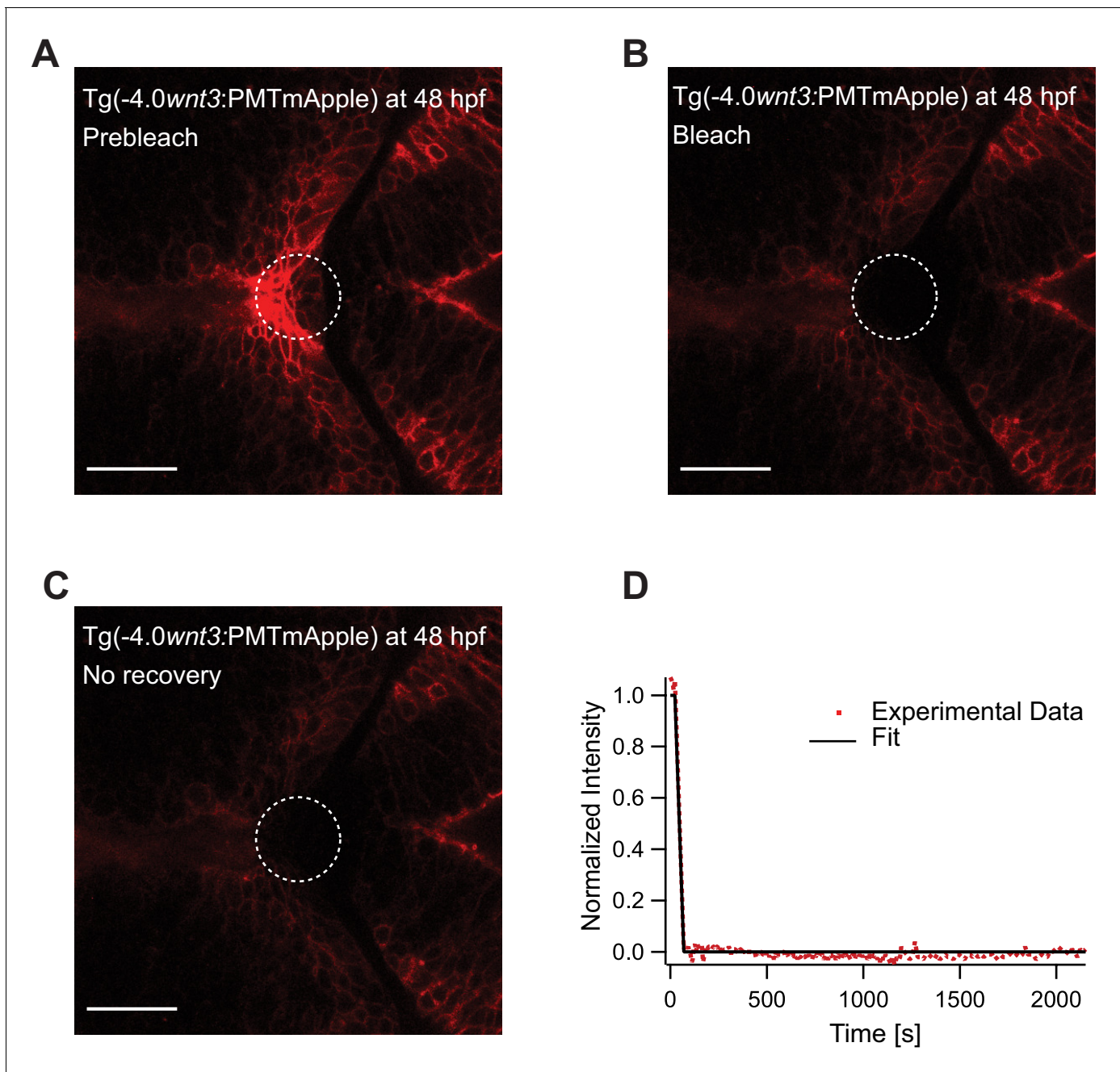


**Figure 5—figure supplement 4.** Representative fluorescence recovery of PMTmApple after photobleaching at 48 hpf. (A) Expression of PMTmApple in Tg(-4.0wnt3:PMTmApple) at 48 hpf before photobleaching. (B) Photobleached region of PMTmApple. (C) No recovery of fluorescence intensity in the bleached region as PMT remains tethered to the cell membrane and does not diffuse. (D) Fluorescence recovery curve for PMTmApple. Images orientation: anterior to the left. Scale bar 30  $\mu$ m.

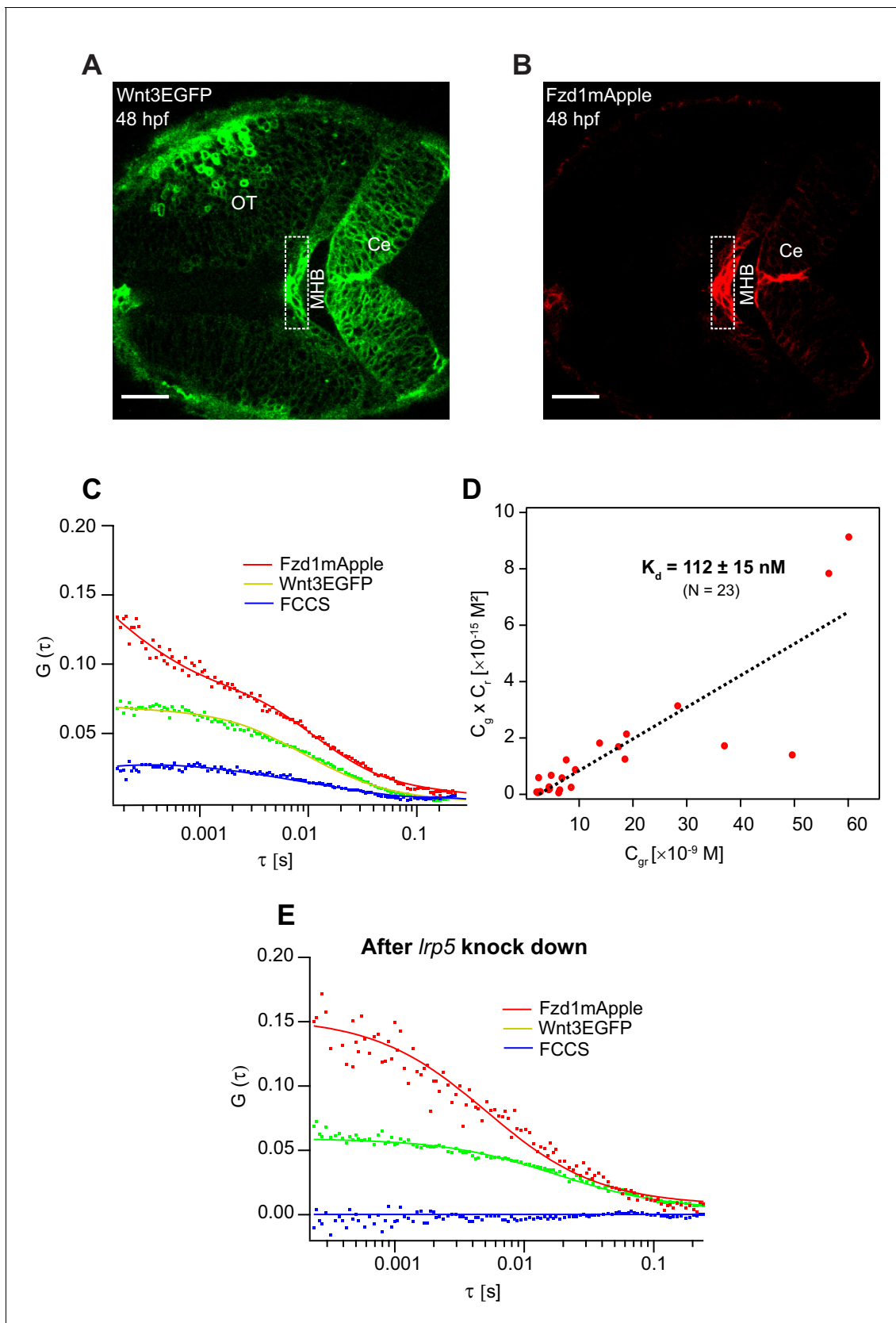


**Figure 6.** Investigation of in vivo Wnt3-Fzd1 binding by FCCS. Expression of (A) Wnt3EGFP and (B) Fzd1mApple in the double transgenic [Tg(−4.0wnt3:Wnt3EGFP)×Tg(−4.0wnt3:Fzd1mApple)] (anterior to the left). (C) Representative auto- and cross-correlation functions (dots) and fittings (lines) of a

Figure 6 continued on next page

## Figure 6 continued

Wnt3EGFP-Fzd1mApple measurement at the indicated region. The cross-correlation function indicates Wnt3EGFP interacts with Fzd1mApple in vivo. (D) Determination of apparent dissociation constant ( $K_d$ ) for Wnt3-Fzd1 interaction in vivo.  $C_g$ ,  $C_r$ , and  $C_{gr}$  represents the concentration of unbound Wnt3EGFP, unbound Fzd1mApple, and bound Wnt3-Fzd1 molecules respectively. The estimated apparent  $K_d$  [ $K_d = (C_g \times C_r)/C_{gr}$ ] for Wnt3-Fzd1 in vivo is  $112 \pm 15$  nM ( $N = 23$ ;  $R^2 = 0.85$ ). (E) Representative auto- and cross-correlation functions (dots) and fittings (lines) of a Wnt3EGFP-Fzd1mApple measurement after knocking down *lrp5*. No cross-correlation indicates Wnt3-Fzd1 interaction is abolished after knockdown of *lrp5*. Scale bars 30  $\mu\text{m}$ .

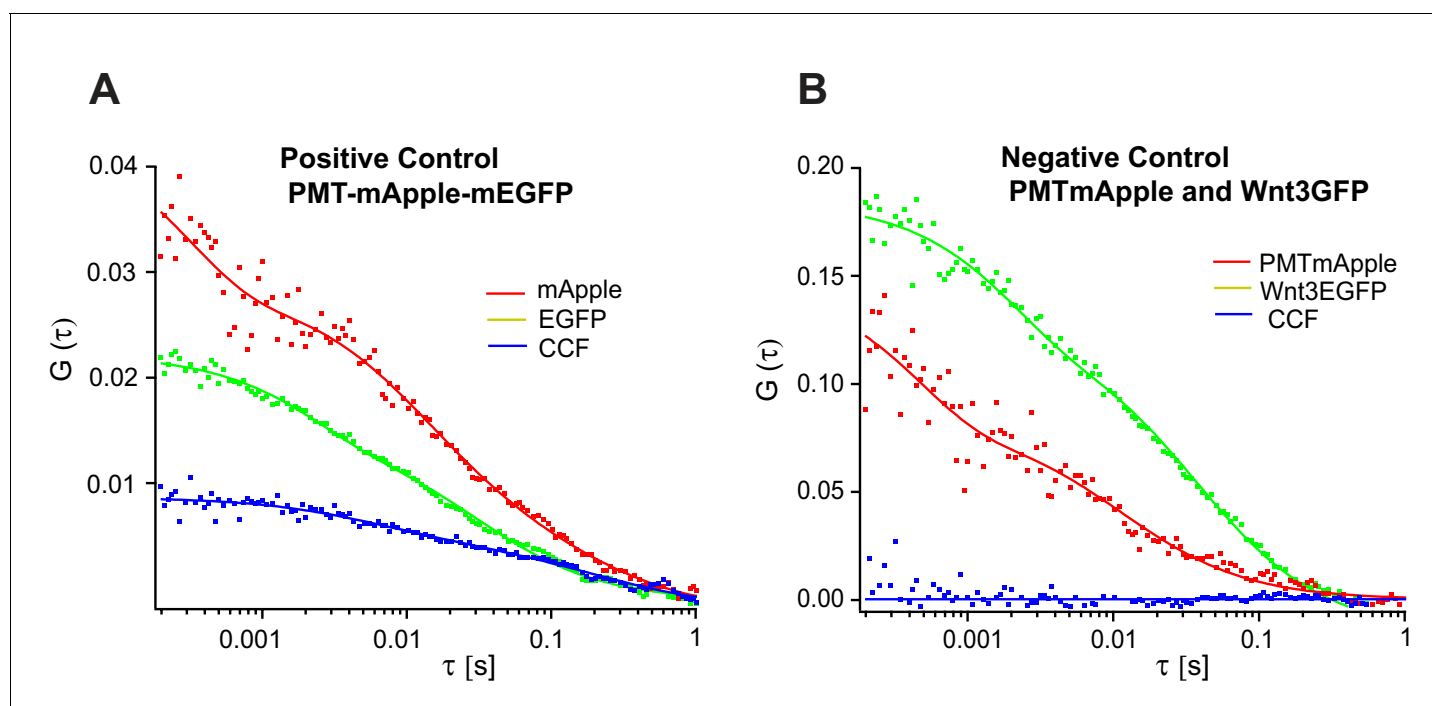


**Figure 6—figure supplement 1.** Representative FCCS measurements for positive and negative control in zebrafish. Representative auto- and cross-correlation functions for (A) PMT-mApple-mEGFP which is a positive control showing a clear cross-correlation and (B) negative control PMT-mApple and Wnt3-EGFP showing no cross-correlations.

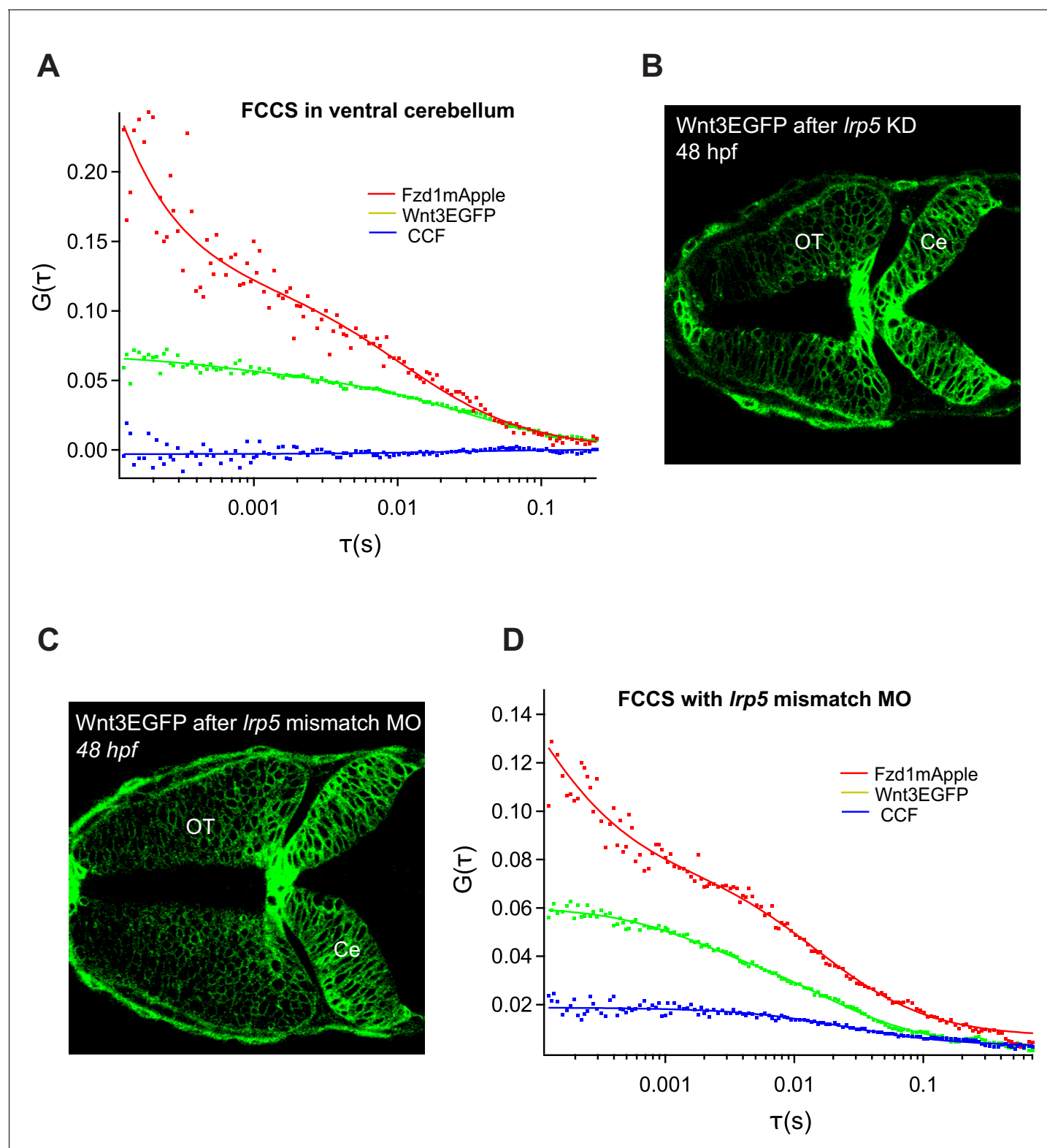


**Figure 6—figure supplement 2.** Role of Lrp5 coreceptor in Wnt3-Fzd1 binding. (A) Representative FCCS measurement for Wnt3EGFP and Fzd1mApple in regions with no Lrp5 expression (ventral cerebellum). No cross-correlations obtained outside midbrain–hindbrain boundary and dorsal cerebellum indicating role of Lrp5 in Wnt3-Fzd1 interaction. (B) Knocking down *Lrp5* morpholino resulting in deformed optic tectum (OT) and cerebellum (Ce) of the zebrafish brain. (C) Wnt3EGFP after treatment with negative control *Lrp5* mismatch MO with five nucleotide substitutions showing normal brain development and (D) retaining cross-correlations between Wnt3EGFP and Fzd1mApple.

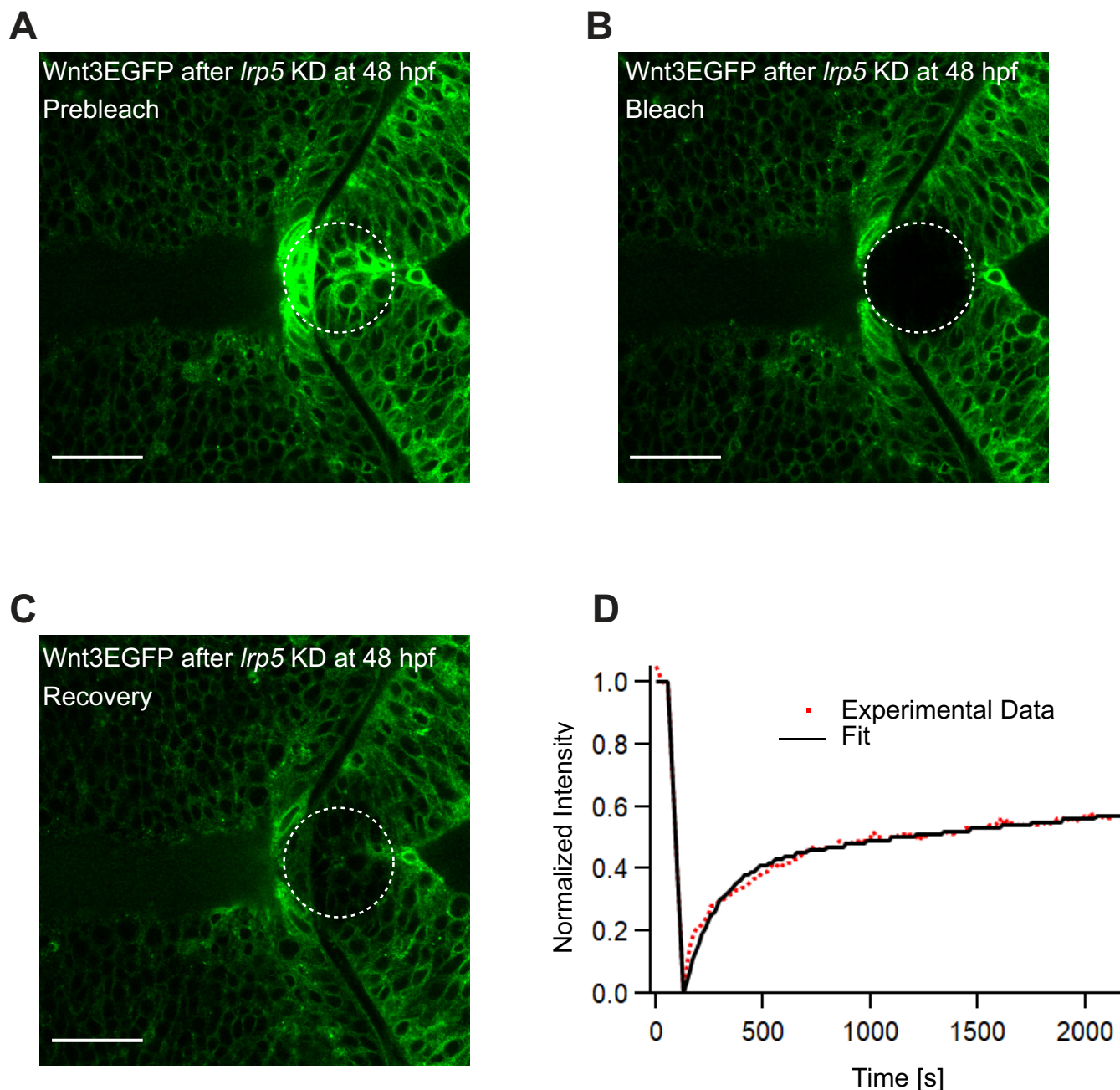


**Figure 6—figure supplement 3.** Representative fluorescence recovery of Wnt3EGFP in *lrp5* knocked-down embryos at 48 hpf after photobleaching. (A) Expression of Wnt3EGFP before photobleaching. (B) Photobleached region of Wnt3EGFP. (C) Recovery of fluorescence intensity in the bleached region due to diffusion of molecules from the neighboring unbleached regions. (D) Fluorescence recovery curve for Wnt3EGFP with a recovery time ( $\tau_{\text{fast}}$ ) of ~150 s and a fraction of mobile component ( $F_m$ ) of ~0.5. The average global diffusion coefficient ( $D_{\text{global}}$ ) measured for Wnt3EGFP after *lrp5* knockdown was  $2.8 \pm 0.8 \mu\text{m}^2/\text{s}$ . Images orientation: anterior to the left. Scale bar 30  $\mu\text{m}$ .